Water Research, Volume 248, January 2024, Article number 120845
DOI:10.1016/j.watres.2023.120845

Quantitative SARS-CoV-2 exposure assessment for workers in wastewater treatment plants using Monte-Carlo simulation

Yi-ning Hu[1,2], Zi-cheng Gui[1,3], Wei-di Wan[1], Tian-nuo Lai[1], Wajid Ali[1], Nian-hong Wan[4], Shan-shan He[4], Sai Liu[5], Xiang Li[6], Zaheer Ahmad Nasir[7], Sonia Garcia Alcega[8], Frederic Coulon[7], Cheng Yan[1,2*]

[1] School of Environmental Studies, China University of Geosciences, Wuhan 430074, PR China
[2] Hubei Key Laboratory of Environmental Water Science in the Yangtze River Basin, China University of Geosciences, Wuhan 430074, PR China
[3] CCDI (Suzhou) exploration and design consultant Co., Ltd., Suzhou 215123, PR China
[4] Central & Southern China Municipal Engineering Design and Research Institute Co, Ltd., Wuhan 430010, PR China
[5] CITIC Treated Water into River Engineering Investment Co., Ltd., Wuhan 430200, PR China
[6] Three Gorges Base Development Co., Ltd., Yichang 443002, PR China
[7] School of Water, Energy and Environment, Cranfield University, Cranfield MK43 0AL, UK
[8] School of Physical Sciences, The Open University, Walton Hall, Milton Keynes MK6 7AA, UK

Corresponding author:
[*]Dr. Cheng Yan
School of Environmental Studies, China University of Geosciences, 388 Lumo Road, Wuhan 430074, PR China
Tel.: +86 027 67883170
Fax: +86 027 67883170
E-mail: cheng_yan@cug.edu.cn

Abstract

Several studies on COVID-19 pandemic have shown that the severe acute respiratory syndrome coronavirus 2 (SARS-CoV-2) originating from human stool are detected in raw wastewater for several days, leading to potential health risks for workers due to the production of bioaerosols and droplets during wastewater treatment process. In this study, data of SARS-CoV-2 concentrations in raw wastewater were gathered from literatures, and a quantitative microbiological risk assessment (QMRA) with Monte Carlo simulation was used to estimate the daily probability of infection risk through exposure to viral airborne particles of the workers during four seasons and under six environmental conditions (hot and humid, hot and dry, mild and humid, mild and dry, cold and humid, and cold and dry). Inhalation of bioaerosols and direct ingestion of wastewater droplets were selected as exposure pathways. Spearman rank correlation coefficients were used for sensitivity analysis to identify the variables with the greatest influence on the infection risk probability. It was found that the daily probability of infection risk decreased with temperature (T) and relative humidity (RH) increase. The probability of direct droplet ingestion pathway was higher than that of the bioaerosol inhalation pathway. The sensitivity analysis indicated that the most sensitive variable for both exposure pathways was the concentration of SARS-CoV-2 in stool. Further to this, the exposure time (t) had a larger variance contribution than T and RH for the bioaerosol inhalation pathway. Implementing measures such as adding more work shifts, mandating personal protective equipment for all workers, and implementing coverage for treatment processes can significantly reduce the risk of infection among workers at WWTPs. These measures are particularly effective during environmental conditions with low temperatures and humidity levels.

Keywords: Daily probability of infection risk; Inhalation of bioaerosols exposure; Direct ingestion of wastewater droplets exposure; wastewater treatment plant; SARS-CoV-2.

1 Introduction

In December 2019, an outbreak of coronavirus disease (COVID-19) unexpectedly occurred in Wuhan, China and spread around the world in a short time (Shi et al., 2020; Tong et al., 2022; WHO, 2020a; 2020b). Given the global pandemic of COVID-19, the World Health Organization announced an international public health emergency on Jan. 30, 2020 (WHO, 2020b). Since then, several studies have shown that viral loads of SARS-CoV-2 RNA have been found in influents and effluents of wastewater treatment plants (WWTPs) all over the world. This is mainly due to the stool of patients being directly discharged into raw sewage (Hata et al., 2020; Rimoldi et al., 2020; Hasan et al., 2021; Saththasivam et al., 2021; Dong et al., 2022; Wang et al., 2022).

The microorganisms and virus contained within the wastewater often end up by being aerosolized during the various treatment processes and become a major source of bioaerosols (Michałkiewicz, 2019). Meanwhile, the rotation of grid machines and aeration of biochemical pools also facilitate the generation of droplets containing pathogenic microorganisms from wastewater (Lou et al., 2021). These bioaerosols and droplets are transmitted by air which is to the main exposure pathway of airborne SARS-CoV-2(Mizukoshi et al., 2021). This is posing a health risk that is at least 1000 times higher than the exposure pathway of contact transmission (Zhang et al., 2022). Hence, it is necessary to investigate the quantitative risks and conduct sensitivity analysis concerning worker exposure to SARS-CoV-2 in WWTPs (Bogler et al., 2020; Gholipour et al., 2021).

However, literatures mainly focused on detecting the gene segment of SARS-CoV-2 RNA in patients' stool or untreated sewage directly in WWTPs (Ahmed et al., 2020; Hart and Halden, 2020; Kweinor Tetteh et al., 2020; Saawarn and Hait, 2021). Furthermore, the meteorological parameters temperature (T) and humidity are considered the main factors affecting the viability of SARS-CoV-2 (Fernández-Raga et al., 2021). Gundy et al. (2009) observed the faster inactivation of 99.9% human coronavirus at 23 °C (within 10 days) compared with that occurring at 4 °C (>100 days). A literature reported that SARS-CoV-2 can survive better in winter than in summer (Kassem, 2020). Lv et al. (2020) reported that the stability of SARS-CoV-2 correlated with T between 4 °C and 70 °C, and its activity was lost at 70 °C within 5 min. Boufekane et al. (2022) stated that decrease in relative humidity (RH) can increase SARS-CoV-2 infection risk. Tong et al. (2022) indicated that the 1% increase in RH was correlated with 1.7%–3.7% increase in infection probability of COVID-19. Although there have been some studies examining the health risks for WWTP workers, there is still a lack of research on the quantitative risks associated with exposure to airborne SARS-CoV-2. In particular, there is a need to investigate the effects of different temperature and humidity conditions on the transmission of SARS-CoV-2 in WWTP environments. Such research is essential for understanding the potential risks to

workers and for developing effective strategies to mitigate those risks. The COVID-19 pandemic has highlighted the importance of protecting essential workers, including those in the wastewater treatment industry, and it is critical that we continue to advance our understanding of the risks associated with their work. By conducting more research on the health risks and sensitivity risks for WWTP workers, we can improve workplace safety and prevent the spread of infectious diseases in these settings. (Usman et al., 2021).

The main objective of this research was to conduct a Monte Carlo simulation-based Quantitative Microbial Risk Assessment (QMRA) to determine the airborne risk of SARS-CoV-2 for workers in small or medium-sized WWTPs. This assessment relied on SARS-CoV-2 concentrations in raw wastewater, as reported in existing literature, and accounted for different exposure scenarios. The study also considered various environmental conditions such as hot and humid, hot and dry, mild and humid, mild and dry, cold and humid, and cold and dry across all four seasons. Additionally, the risk associated with the direct ingestion of droplets from wastewater was also analyzed. In addition, Spearman rank correlation coefficients were used to quantitatively weigh the contributions of inputted variable parameters by sensitivity analysis. This study contributes novel insights into seasonal and regional variations of infection risks of airborne SARS-CoV-2 among WWTP workers to support stakeholders in mitigating the health risks of sewage workers during the prolonged global pandemic of COVID-19.

2 Method and materials

2.1 Acquisition of SARS-CoV-2 data

To summarize the SARS-CoV-2 concentrations in wastewater across various regions, a structured review of the literature was conducted. The regions covered in the review included South America, Asia, Europe, Australia, North Africa, and the United States. The review was conducted using two databases, namely ScienceDirect and Web of Science. Additional information regarding the review process can be found in Supplementary Material Figure 1. The study also utilized Supplementary Material Table 1 to reference the data on SARS-CoV-2 concentrations in stool. For the purpose of the study, the worst-case scenario was considered, and it was assumed that the SARS-CoV-2 concentration in stool was between 1.7×10^6 and 4.1×10^7 genomes per mL, as reported by Han et al. in 2020. All the computing methods and parameters used for the Quantitative Microbial Risk Assessment (QMRA) were detailed in Table 1. SARS-CoV-2 in wastewater was considered from the stool of COVID-19 patients (Heller et al., 2020; Zaneti et al., 2021). The amount of SARS-CoV-2 in stools of each patient (S_v) was calculated using Equation (1):

$$S_v = c \times v \qquad (1)$$

where c is the concentration of SARS-CoV-2 in the stool of patients, and v is the volume

of stool equals the weight of stool divided by stool density.

The daily concentration of SARS-CoV-2 in wastewater (C_{in}) was calculated using Equation (2) (Dada and Gyawali, 2021):

$$C_{in} = \frac{P_p \times S_v \times F}{V_S} \quad (2)$$

where P_P is the proportion of patients among the population served by WWTPs during the COVID-19 pandemic; F is the proportion of patients having SARS-CoV-2 in stool; V_s is the amount of daily wastewater discharge of per person served by the WWTPs.

2.2 QMRA framework

2.2.1 Hazard identification

The COVID-19 pandemic has presented new challenges for the wastewater treatment industry. Evidence has shown that the RNA load of SARS-CoV-2 has been detected in wastewater due to the direct discharge of COVID-19 patient stool into sewers (Randazzo et al., 2020). As a result, workers in wastewater treatment plants (WWTPs) are at risk of exposure to airborne SARS-CoV-2 during their daily work routines. This is a major concern as WWTP workers are essential to maintaining the safety and sanitation of our water supply. The risk of infection for WWTP workers is further exacerbated by the nature of their work, which involves proximity to raw wastewater and its associated bioaerosols (Chen et al., 2021). Therefore, it is crucial to identify effective measures to reduce the risk of infection among these workers. This highlights the importance of conducting research into the quantitative health risks and sensitivity risks associated with worker exposure to airborne SARS-CoV-2, as well as exploring strategies to mitigate these risks.

2.2.2 Exposure assessment

The treatment processes can produce bioaerosols and wastewater droplets, which have the greatest potential risk for workers in WWTPs (Haji Ali et al., 2021). Thus, this study employed two exposure pathways (inhalation of bioaerosols and direct ingestion of wastewater droplets) to evaluate the dose of SARS-CoV-2 exposure of WWTP workers. Table 1 lists the specific values of the parameters for QMRA calculations.

For bioaerosol inhalation exposure pathway, the dose of SARS-CoV-2 ingestion of workers was varied per day. The viability of aerosolized SARS-CoV-2 in this pathway was affected greatly by T and humidity (relative and absolute humidity) (Del Rio and Camacho-Ortiz, 2020). Thus, to analyze this influence in various environmental conditions, six types of environmental conditions (hot and humid, hot and dry, mild and humid, mild and dry, cold and humid, and cold and dry) in four seasons were studied with a focus on their diverse humidity and T (Supplementary Material Tables 2 and 3).

Table 1. Computing methods and parameters for QRMA

Items	Description	Unit	Values	References
C_{in}	Daily initial concentration of SARS-CoV-2 in wastewater $C_{in} = \frac{P_p \times S_v \times F}{V_s}$	PFU m^{-3}	By calculation	-
P_p	The proportion of people getting the COVID-19 served by a wastewater treatment plant	%	Best-case scenario: P_p= 0.03 Worst-case scenario: P_p= 3	Dada and Gyawali, 2021
S_v	The amount of SARS-CoV-2 in the stools of per infected person $S_v = c \times v$	PFU	By calculation	-
c	Concentrations of SARS-CoV-2 in stool of infected person in wastewater	PFU mL^{-1}	c = 1.7×10^6 ~ 4.1×10^7 (genomes/ mL)	Supplementary Material Table 1
			1000 genomes = 1 PFU	Jensen et al., 2018
v	Volume of stool $v = \frac{m}{\rho}$	ml	Weight of stool: m=200 g	Wu et al., 2020
			Density of stool: ρ = 1.06 ~ 1.09 g/mL	Penn et al., 2018
F	The proportion of infected people had SARS-CoV-2 in stool	%	48.1	Cheung et al., 2020
V_s	Daily wastewater discharge loading per person	m^3	V_s=0.25	Wang et al., 2011
d	Exposure dose	PFU	By calculation	Dada and Gyawali, 2021
	Modeling: $d = (1-\alpha) \times C_{in} \times V_a \times IR \times t \times ag$			

	Direct ingest: $d = I \times C_{in}$		Wastewater volume ingested: I=1 ml	Zaneti et al., 2021 Westrell et al., 2004
α	Filtration efficiency of a N95-mask	%	95	Haas et al., 2017
V_a	Viability of aerosolized SARS-CoV-2 $V_a = -0.0515 \times AH + 2.0487$	%	By calculation	Marr et al., 2019
AH	Absolute humidity $AH = \frac{1322.7 \times exp\,(17.625 \times \frac{T}{T+243.04}) \times \frac{RH}{100}}{T+273.15}$	g m^{-3}	By calculation	Marr et al., 2019
T	Centigrade degree	°C	-	Supplementary Material Table 2
RH	Relative humidity	%	-	Supplementary Material Table 3
IR	Inhaled breathing rate	m^3 h^{-1}	Male: IR=0.78, Female: IR=0.62	Ministry of Environmental Protection, 2013
t	Exposure time	min d^{-1}	t=5~10	-
ag	Aerosol ingestion rate	%	50	Jahne et al., 2015
$P_i(d)$	Probability of infection after a daily exposure Exponential dose-response model: $P_i(d) = 1 - e^{-d/k}$	-	$k=4.1\times10^2$	Watanabe et al., 2010

Absolute humidity (*AH*) was calculated by Equation (3) (Marr et al., 2019):

$$AH = \frac{1322.7 \times exp\,(17.625 \times \frac{T}{T+243.04}) \times \frac{RH}{100}}{T+273.15} \quad (3)$$

where *T* is the temperature in centigrade degree, and *RH* is relative humidity (%).

The viability of aerosolized SARS-CoV-2 (V_a) was computed by Equation (4) (Marr et al., 2019):

$$V_a = -0.0515 \times AH + 2.0487 \quad (4)$$

The exposure dose of the bioaerosol inhalation exposure pathway was calculated using Equation (5) (Dada and Gyawali, 2021):

$$d = (1-\alpha) \times C_{in} \times V_a \times IR \times t \times ag \quad (5)$$

where α is the filtration efficiency of a N95-mask; *IR* is inhaled breathing rate of workers; *t* is exposure time of workers in WWTPs; *ag* is the aerosol ingestion rate.

The other exposure pathway is direct ingestion of wastewater droplets. For this pathway, the workers were assumed to ingest 1 mL wastewater directly. The exposure dose of this pathway was computed using Equation (6) (Westrell et al., 2004; Zaneti et al., 2021):

$$d = I \times C_{in} \quad (6)$$

where *I* is the wastewater volume ingestion of workers, i.e., 1 ml.

2.2.3 Dose-response model and risk characterization

The dose-response relationship is the quantitative relationship between the levels of risk and dose (Haas, 2015). Although, no ready-made dose-response relationship for SARS-CoV-2 is available, Watanabe et al. (2010) proposed an exponential dose-response model for SARS-CoV-1. Sarkar et al. (2021) observed that SARS-CoV-2 sequence in human host was approximately 76.59% similar to the SARS-CoV-1 sequence. Corpuz et al. (2020) stated that SARS-CoV-1 and SARS-CoV-2 have structural similarities. van Doremalen et al. (2020) reported that the does-response model for SARS-CoV-2 can be assumed to be the same as that for SARS-CoV-1 because of the similarities in their structure and epidemiological characteristics.

Thus, this study employed an exponential dose-response model to determine the associations between the exposure dose and health risk. The probability of infection after a daily exposure was determined using Equation (7) (Watanabe et al., 2010):

$$P_i(d) = 1 - e^{-d/k} \quad (7)$$

where *k* is the probability of infection after a daily exposure (Table 1).

2.3 Monte Carlo simulation and sensitivity analysis

All input variable parameters (concentrations of SARS-CoV-2 in stool, stool density, exposure time, *T*, and *RH*) in QMRA were randomly selected from their probability distributions. According to Haas (2020), Quantitative Microbial Risk Assessment (QMRA) is a valuable tool for analyzing health risks associated with SARS-CoV-2 in various exposure scenarios. Based on this, QMRA was utilized in the present study as a quantitative method for assessing the health risks faced by WWTP workers. Through the application of QMRA, the study was able to identify and quantify potential risks to WWTP workers and propose effective strategies for mitigating those risks. Such

quantitative risk analysis is essential for protecting the health and safety of essential workers during the ongoing COVID-19 pandemic. By using Microsoft Excel 2013 and Oracle Crystal Ball, output daily probability of infection risk was calculated with 10,000 iterations to reach the steady-state distributions (Shi et al., 2018). The results of Monte Carlo simulation were revealed by box-and-whiskers charts.

Spearman rank correlation coefficient and contribution to variance were assessed using sensitivity analysis with Oracle Crystal Ball. For bioaerosol inhalation exposure pathway, the input variables were the concentrations of SARS-CoV-2 in the stool, exposure time, *T*, *RH*, and stool density. For direct droplet ingestion exposure pathway, the input variables were concentrations of SARS-CoV-2 in stool and stool density. The output variable for both exposure pathways was the daily infection probability of SARS-CoV-2. The results were visualized in tornado plots. The higher the Spearman rank correlation coefficients, the greater the contribution of the corresponding input values. Contributions to variance were displayed by values in the range of 0% to 100%, and they were calculated by squaring and normalizing the rank correlation coefficient to 100% (Zhou et al., 2014; Haas et al., 2017; Shi et al., 2018). The higher the percentage of contribution to variance, the higher the relative importance of the input variables.

3. Results and discussion

3.1 Health risks for inhalation of bioaerosols

Figure 1 presents the daily probability of infection for different exposure scenarios, considering the bioaerosol inhalation exposure pathway, across six different environmental conditions for both males and females. The findings indicate that for females, the probability of infection was 1.3 times lower in hot and mild, and 1.2 lower in cold environmental conditions, when compared to males. This difference in risk can be attributed to the fact that males have a faster inhalation rate compared to females (as shown in Table 1). Our results are consistent with those reported by Azzolina et al. (2020), who found that males had a higher rate and anticipation in the epidemic curve compared to females. Similarly, Pérez-López et al. (2020) reported that the COVID-19 mortality rate was higher among males compared to females in European countries. These findings underscore the importance of considering gender-specific differences in the risk of infection and the need for implementing appropriate measures to protect both male and female workers in WWTPs.

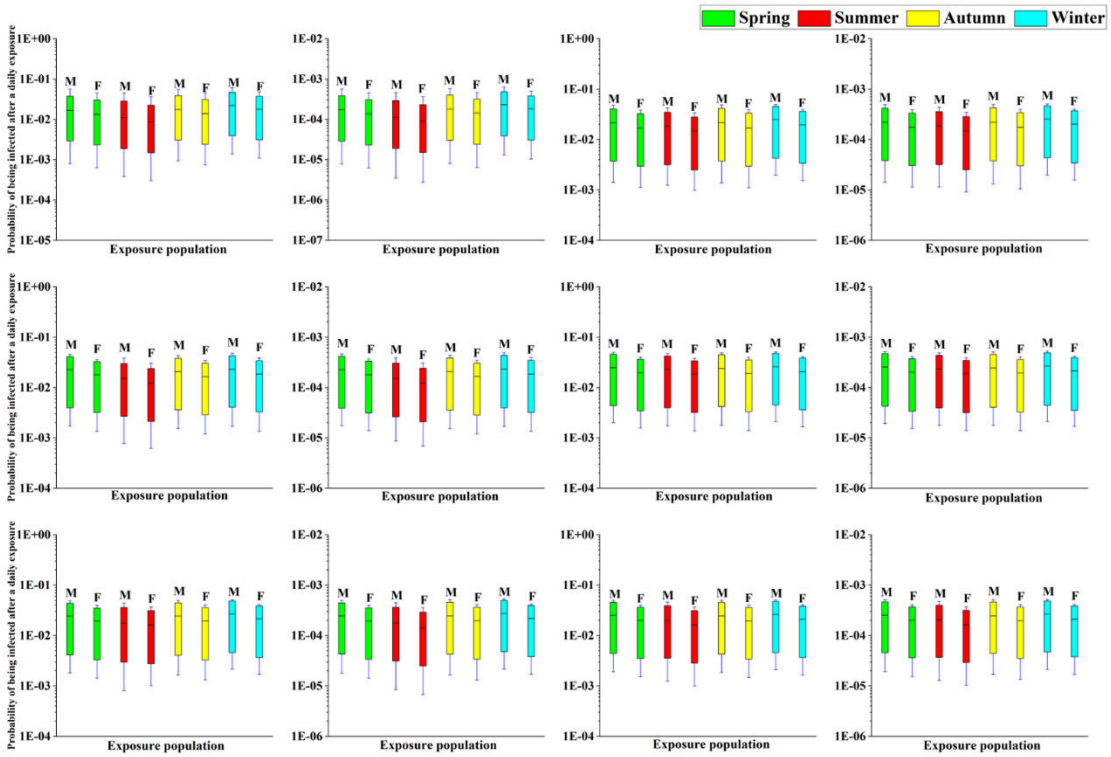

Figure 1. Daily probability of infection (*Pi(d)*) for the bioaerosol inhalation pathway of various exposure scenarios in four seasons referring to six kinds of environmental conditions: (a) worst-case scenario for hot and humid conditions, (b) best-case scenario for hot and humid conditions, (c) worst-case scenario for hot and dry conditions, (d) best-case scenario for hot and dry conditions, (e) worst-case scenario for mild and humid conditions, (f) best-case scenario for mild and humid conditions, (g) worst-case scenario for mild and dry conditions, (h) best-case scenario for mild and dry conditions, (i) worst-case scenario for cold and humid conditions, (j) best-case scenario for cold and humid conditions, (k) worst-case scenario for cold and dry conditions, and (l) best-case scenario for cold and dry conditions. (The bottom and top of the box respectively represent the first and third quartiles (25th and 75th percentile values), the band inside the box denotes the second quartile (median), and the tetragon inside the box refers to the average value. The bottom and top of the whiskers respectively represent the 5th percentile values and 95th percentile values; M for Male, F for Female).

In all three types of environmental conditions (hot, mild, and cold), the worst-case scenario exhibited an infection probability that was approximately two orders of magnitude higher (ranging from 6.92×10^{-6} to 5.28×10^{-4}) compared to the best-case scenario (ranging from 6.16×10^{-4} to 5.15×10^{-2}). This emphasizes the significant impact of environmental conditions on the risk of infection and the need for appropriate measures to be taken to minimize the risks for WWTP workers. This finding is in agreement with the fact that the proportion of people infected under the best-case scenario was two orders of magnitudes higher than that of people in the worst-case scenario (Table 1). Similar findings were reported by Dada and Gyawali (2021),

indicating that the infection risk during a low-grade outbreak was significantly lower compared to an aggressive outbreak during the COVID-19 pandemic. Compared with hot environment conditions (2.77×10^{-6} to 6.06×10^{-2}), the infection risk was the higher in cold environment conditions (9.12×10^{-6} to 5.15×10^{-2}). Usually, virus survival decreases as *T* increases (Polozov et al. 2008). Mandal et al. (2020) found a negative relationship between *T* and COVID-19 cases. Haque and Rahman (2020) declared that the high *T* can minimize SARS-CoV-2 viability. Wang et al. (2021) reported the robust negative correlation between SARS-CoV-2 transmissibility and *T* (or *RH*) in China and U.S.

Figures 1a-d show that during hot environmental conditions, the probability of infection was highest in winter (1.04×10^{-5} to 6.06×10^{-2}) and lowest in summer (2.77×10^{-6} to 4.55×10^{-2}). This finding can be attributed to the fact that SARS-CoV-2 is more viable in winter and less viable in summer due to temperature differences (Kassem, 2020). In addition, the probability of infection was consistently higher in dry environmental conditions (9.12×10^{-6} to 4.95×10^{-2}) (Figs. 1c and 1d) compared to humid environmental conditions (2.77×10^{-6} to 6.06×10^{-2}) (Figs. 1a and 1b), which is consistent with the reduced transmission of SARS-CoV-2 in high humidity conditions (Haque and Rahman, 2020). Boufekane et al. (2022) also reported a negative correlation between relative humidity and new cases of COVID-19.

For mild environmental conditions (Figs. 1e-h), the probability of infection was highest in winter (1.14×10^{-4} to 4.74×10^{-2}) and lowest in summer (5.29×10^{-5} to 4.30×10^{-2}), with slightly higher values in spring (7.80×10^{-5} to 4.48×10^{-2}) than in autumn (7.35×10^{-5} to 4.03×10^{-2}). In dry environmental conditions (Figs. 1g, 1h, 1k, and 1l), the probability of infection was 0.09-0.56 times higher than in humid environmental conditions (Figs. 1e, 1f, 1i, and 1j).

For cold environmental conditions, the probability of infection peaked in winter (1.69×10^{-5} to 5.16×10^{-2}) and was lowest in summer (6.75×10^{-6} to 4.62×10^{-2}), with similar values in spring (1.42×10^{-5} to 5.00×10^{-2}) and autumn (1.31×10^{-5} to 5.04×10^{-2}). Compared to humid environmental conditions, dry environmental conditions had 0.04-0.25 and 0.02-0.20 times higher probability of infection in spring and summer, respectively, but 0.001-0.03 times lower values in winter. This result is explained by the combination of relative humidity and temperature, where temperature has a greater impact on the probability of infection than relative humidity in cold environmental conditions during winter (Marr et al., 2019).

3.2 Health risks for direct ingestion of wastewater droplets

Figure 2 indicates the daily probability of infection of the direct droplet ingestion exposure pathway. The infection risk of the worst-case scenario (4.46×10^{-3} to 1.02×10^{-1}) was about two orders of magnitudes larger than that of the best-case scenario (4.47×10^{-5} to 1.07×10^{-3}).

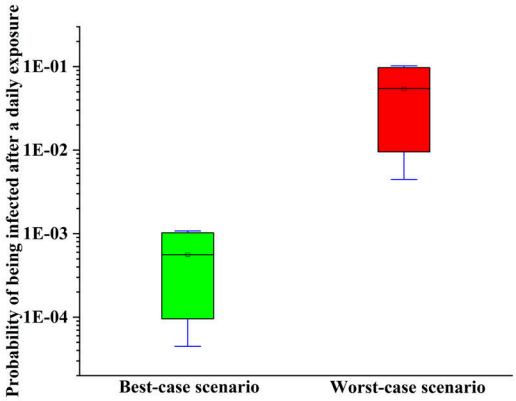

Figure 2. Daily probability of infection ($P_i(d)$) for the direct droplet ingestion pathway. (The bottom and top of the box respectively represent the first and third quartiles (25th and 75th percentile values), the band inside the box denotes the second quartile (median), and the tetragon inside the box refers to the average value. The bottom and top of the whiskers respectively represent the 5th percentile values and 95th percentile values).

This result is related to the different proportions of infected people between the two scenarios (Table 1). However, compared with the exposure pathway of bioaerosol inhalation (Supplementary Material Table 4), the probability of infection of the direct droplet ingestion exposure pathway was 1.04–5.29 times higher because of the condition in which all SARS-CoV-2 should be alive in the ingested droplets, which increased the exposure dose (Table 1). Thus, the direct droplet ingestion exposure pathway should be more conservative than the bioaerosol inhalation exposure pathway. Zaneti et al. (2021) reported similar results. They used the direct droplet ingestion exposure pathway and reckoned that it was a conservative QMRA approach to assume viable SARS-CoV-2 in wastewater for the assessment of the risk of infection.

3.3 Sensitivity analysis

3.3.1 Inhalation of bioaerosols

Figure 3 shows the ranking of input variables for the sensitivity of bioaerosol inhalation for the six kinds of environmental conditions during four seasons.

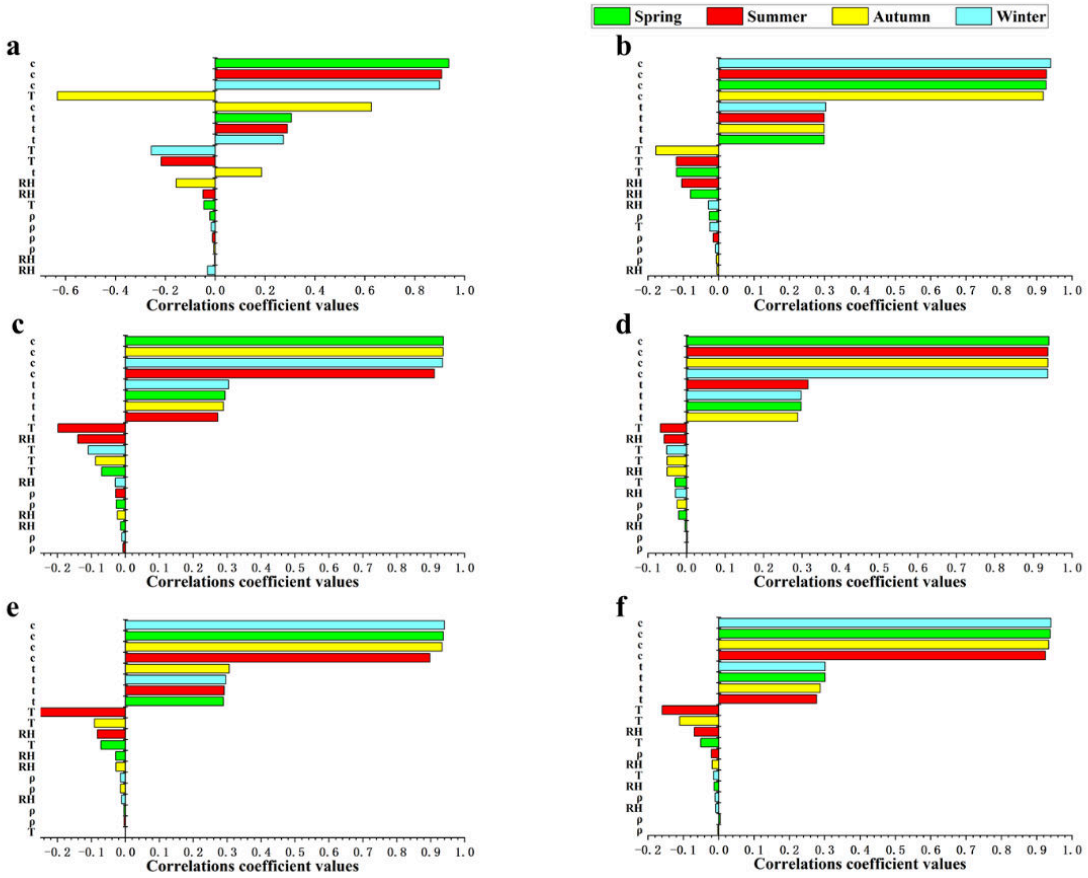

Figure 3. Tornado charts showing the ranking of input variables that impact the output values of daily infection risk for the bioaerosol inhalation pathway in four seasons referring to six kinds of environmental conditions: (a) hot and humid conditions, (b) hot and dry conditions, (c) mild and humid conditions, (d) mild and dry conditions, (e) cold and humid conditions, and (f) cold and dry conditions. (*c*: Concentrations of SARS-CoV-2 in stool; *t*: Exposure time; *T*: Temperature; *RH*: Relative humidity; ρ: Density of stool).

Supplementary Material Figure 1 provides the sensitivity percentage of each input variable. The sensitivity of variables showed almost the same pattern in six types of environmental conditions in four seasons. The ranking of input variables indicated that the concentration of SARS-CoV-2 in stool (*c*) was the most sensitive input value, regardless of seasons or environmental conditions (Fig. 3). The contribution to variance of concentration of SARS-CoV-2 in stool (*c*) accounted for 39% to 75%, and it provided the largest contribution for the six different environmental conditions in four seasons (Supplementary Material Fig. 1). To minimize exposure to SARS-CoV-2 bioaerosols, it is crucial to implement effective measures and maintain low and short-lasting exposure times, as recommended by Kataki et al. (2021). In wastewater treatment plants (WWTPs), appropriate aeration methods and aerator types such as submerged aeration, underwater aeration, coarse bubble aeration, and diffused aeration systems can significantly reduce bioaerosol generation (Fernando and Fedorak, 2005; Sanchez-

Monedero et al., 2008; Korzeniewska, 2011). Covering the primary clarifier weir area and aeration chambers in WWTPs can also decrease bioaerosol dispersion (Korzeniewska et al., 2009; Fathi et al., 2017). Similarly, in indoor working areas such as sludge dewatering houses, effective ventilation can significantly reduce bioaerosol concentrations (Guo et al., 2014). Exposure time (t) ranked second in the contribution to daily infection risk (Fig. 3). The fraction of the contribution to variance of exposure time accounted for 12% to 24%, and it showed a slight difference among four seasons in six kinds of environmental conditions (Supplementary Material Fig. 1). Carducci et al. (2016) verified an increased trend of probability of infection as a function of exposure time. Gholipour et al. (2021) also considered that a reduction in working hours, i.e., exposure time, can decrease the infection risks of SARS-CoV-2 for WWTP workers. Therefore, increasing the number of shifts for the workers in WWTPs should be an effective way to reduce the risk of COVID-19 infection.

Furthermore, T and RH had a crucial effect on the viability of SARS-CoV-2 and is important for its infection probability. The ranking of input variables showed that both were inversely proportional to infection probability (Fig. 3). Briz-Redón and Serrano-Aroca (2020) manifested a negative correlation between SARS-CoV-2 infection incidence and T and RH in most exposure scenarios. The contribution fraction of T (1.15% to 38.87%) was higher than that of RH (0.02% to 9.79%) (Supplementary Material Fig. 1). Meanwhile, the contributions of these input variables were higher in summer and humid environmental conditions (Supplementary Material Fig. 1). Therefore, avoiding low T and RH should be one of the most effective methods to decrease the probability of infection in summer and humid environmental conditions.

3.3.2 Direct ingestion of wastewater droplets

Figure 4 shows the ranking of input variables for the sensitivity of direct droplet ingestion pathway under different scenarios. Supplementary Material Figure 2 displays the sensitivity percentage of each input variable. Two input variables were used for direct droplet ingestion pathways: concentration of SARS-CoV-2 in stool (c) and stool density (ρ). The results of sensitivity analysis showed that the concentration of SARS-CoV-2 in stool was the leading factor for daily infection probability (Fig. 4). The Spearman rank correlation coefficient was approximately 66 times higher than the stool density (Fig. 4). In addition, the percentage of variance contribution of the concentration of SARS-CoV-2 in stool was 98.51% proportional to the infection probability, whereas stool density was 1.49% inversely proportional to the infection probability (Supplementary Material Fig. 2).

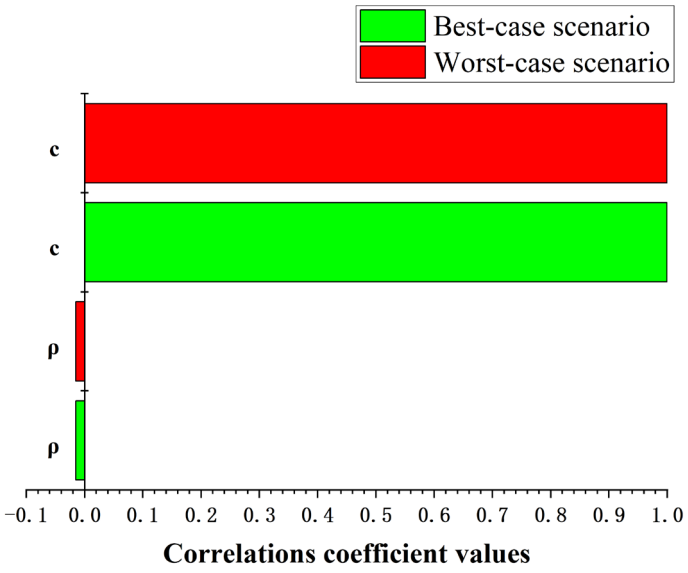

Figure 4. Tornado chart showing the ranking of input variables that impact the output values for the direct droplet ingestion pathway. (*c*: Concentrations of SARS-CoV-2 in stool; *ρ*: Density of stool).

4 Conclusion

The daily probability of infection via the bioaerosol inhalation pathway was higher in males than in females, due to the higher breath rate of males. Additionally, cold and dry environmental conditions were found to pose a higher risk of infection than hot and humid conditions, with winter being the season with the highest risk. This was attributed to the negative correlation between the viability of SARS-CoV-2 and temperature and relative humidity. In particular, in cold and dry conditions, humid conditions increased the probability of infection. The worst-case scenario for both bioaerosol inhalation and direct droplet ingestion pathways presented a much higher risk of infection compared to the best-case scenario. The direct droplet ingestion pathway posed a higher risk due to the viability of SARS-CoV-2 in the ingested droplets. However, for the bioaerosol inhalation pathway, the concentration of SARS-CoV-2 in stool and exposure time were found to be the most significant contributors to the daily infection risk, while temperature and relative humidity had a smaller influence. In both exposure pathways, the concentration of SARS-CoV-2 in stool was the most sensitive variable. The study provides valuable insights for regulators and decision makers in local sewage utilities to develop policies and management measures to reduce the health risk of sewage workers during the ongoing COVID-19 pandemic.

CRediT authorship contribution statement

Yi-ning Hu: Conceptualization, Data curation, Writing-original draft, Writing-review & editing, Visualization, Software. Zi-cheng Gui: Writing-original draft, Visualization, Software, Supervision & Validation. Wei-di Wan: Software, Supervision & Validation. Tian-nuo Lai: Visualization, Software. Wajid Ali: Software, Supervision & Validation, Writing-review & editing. Nian-hong Wan: Software, Supervision & Validation, Writing-review & editing. Shan-shan He: Software, Supervision & Validation, Writing-review & editing. Sai Liu: Software, Supervision & Validation, Writing-review & editing. Xiang Li: Conceptualization, Visualization, Software. Zaheer Ahmad Nasir: Supervision & Validation, Writing-review & editing. Sonia Garcia Alcega: Supervision & Validation, Writing-review & editing. Frederic Coulon: Funding acquisition, Writing-review & editing, Visualization, Supervision & Validation. Cheng Yan: Funding acquisition, Conceptualization, Data curation, Writing-original draft, Writing-review & editing, Visualization, Software, Investigation, Resources, Supervision & Validation.

Declaration of Competing Interest

The authors declare that they have no known competing financial interests or personal relationships that could have appeared to influence the work reported in this paper.

Acknowledgments

This study was sponsored by the National Natural Science Foundation of China (51608497) and supported through the Environmental Microbiology and Human Health Programme (Grant Reference NE/M010961/1) and SPF Clean Air Programme Grant NE/V002171/1. All data supporting this study are included within the article and supporting materials.

References

Ahmed, W., Angel, N., Edson, J., Bibby, K., Bivins, A., O'Brien, J.W., Choi, P.M., Kitajima, M., Simpson, S.L., Li, J., Tscharke, B., Verhagen, R., Smith, W.J.M., Zaugg, J., Dierens, L., Hugenholtz, P., Thomas, K.V., Mueller, J.F., 2020. First confirmed detection of SARS-CoV-2 in untreated wastewater in Australia: A proof of concept for the wastewater surveillance of COVID-19 in the community. Sci. Total Environ. 728, 138764. https://doi.org/10/ggs449

Anjos, D., Fiaccadori, F.S., Servian, C. do P., da Fonseca, S.G., Guilarde, A.O., Borges, M.A.S.B., Franco, F.C., Ribeiro, B.M., Souza, M., 2022. SARS-CoV-2 loads in urine, sera and stool specimens in association with clinical features of COVID-19

patients. J. Clin. Virol. Plus 2, 100059. https://doi.org/10.1016/j.jcvp.2021.100059
Azzolina, D., Magnani, C., Gallo, E., Ferrante, D., Gregori, D., 2020. Gender and age factors affecting the mortality during the COVID-19 epidemic in Italy. Epidemiol. Prev. 44, 252–259. https://doi.org/10/gqmb6s
Bogler, A., Packman, A., Furman, A., Gross, A., Kushmaro, A., Ronen, A., Dagot, C., Hill, C., Vaizel-Ohayon, D., Morgenroth, E., Bertuzzo, E., Wells, G., Kiperwas, H.R., Horn, H., Negev, I., Zucker, I., Bar-Or, I., Moran-Gilad, J., Balcazar, J.L., Bibby, K., Elimelech, M., Weisbrod, N., Nir, O., Sued, O., Gillor, O., Alvarez, P.J., Crameri, S., Arnon, S., Walker, S., Yaron, S., Nguyen, T.H., Berchenko, Y., Hu, Y., Ronen, Z., Bar-Zeev, E., 2020. Rethinking wastewater risks and monitoring in light of the COVID-19 pandemic. Nat. Sustain. 3, 981–990. https://doi.org/10/gh75xw
Boufekane, A., Busico, G., Maizi, D., 2022. Effects of temperature and relative humidity on the COVID-19 pandemic in different climates: a study across some regions in Algeria (North Africa). Environ. Sci. Pollut. Res. 29, 18077–18102. https://doi.org/10/gqmb6m
Briz-Redón, Á., Serrano-Aroca, Á., 2020. The effect of climate on the spread of the COVID-19 pandemic: A review of findings, and statistical and modelling techniques. Prog. Phys. Geogr. Earth Environ. 44, 591–604. https://doi.org/10/gg7m99
Carducci, A., Donzelli, G., Cioni, L., Verani, M., 2016. Quantitative Microbial Risk Assessment in Occupational Settings Applied to the Airborne Human Adenovirus Infection. Int. J. Environ. Res. Public. Health 13, 733. https://doi.org/10.3390/ijerph13070733
Chen, Y., Yan, C., Yang, Y., Ma, J., 2021. Quantitative microbial risk assessment and sensitivity analysis for workers exposed to pathogenic bacterial bioaerosols under various aeration modes in two wastewater treatment plants. Sci. Total Environ. 755, 142615. https://doi.org/10.1016/j.scitotenv.2020.142615
Cheung, K.S., Hung, I.F.N., Chan, P.P.Y., Lung, K.C., Tso, E., Liu, R., Ng, Y.Y., Chu, M.Y., Chung, T.W.H., Tam, A.R., Yip, C.C.Y., Leung, K.-H., Fung, A.Y.-F., Zhang, R.R., Lin, Y., Cheng, H.M., Zhang, A.J.X., To, K.K.W., Chan, K.-H., Yuen, K.-Y., Leung, W.K., 2020. Gastrointestinal Manifestations of SARS-CoV-2 Infection and Virus Load in Fecal Samples From a Hong Kong Cohort: Systematic Review and Meta-analysis. Gastroenterology 159, 81–95. https://doi.org/10/ggrqjr
Corpuz, M.V.A., Buonerba, A., Vigliotta, G., Zarra, T., Ballesteros, F., Campiglia, P., Belgiorno, V., Korshin, G., Naddeo, V., 2020. Viruses in wastewater: occurrence, abundance and detection methods. Sci. Total Environ. 745, 140910. https://doi.org/10/gg5xv4
Dada, A.C., Gyawali, P., 2021. Quantitative microbial risk assessment (QMRA) of occupational exposure to SARS-CoV-2 in wastewater treatment plants. Sci. Total Environ. 763, 142989. https://doi.org/10/gm4ms8
Del Rio, C., Camacho-Ortiz, A., 2020. Will environmental changes in temperature affect the course of COVID-19? Braz. J. Infect. Dis. 24, 261–263. https://doi.org/10/ggv2hw

Dong, Q., Cai, J.-X., Liu, Y.-C., Ling, H.-B., Wang, Q., Xiang, L.-J., Yang, S.-L., Lu, Z.-S., Liu, Y., Huang, X., Qu, J.-H., 2022. Occurrence and decay of SARS-CoV-2 in community sewage drainage systems. Engineering S2095809922002247. https://doi.org/10/gqrgd8

Fathi, S., Hajizadeh, Y., Nikaeen, M., Gorbani, M., 2017. Assessment of microbial aerosol emissions in an urban wastewater treatment plant operated with activated sludge process. Aerobiologia 33, 507–515. https://doi.org/10.1007/s10453-017-9486-2

Fernández-Raga, M., Díaz-Marugán, L., García Escolano, M., Bort, C., Fanjul, V., 2021. SARS-CoV-2 viability under different meteorological conditions, surfaces, fluids and transmission between animals. Environ. Res. 192, 110293. https://doi.org/10/ghmtrk

Fernando, N.L., Fedorak, P.M., 2005. Changes at an activated sludge sewage treatment plant alter the numbers of airborne aerobic microorganisms. Water Res. 39, 4597–4608. https://doi.org/10.1016/j.watres.2005.08.010

Gholipour, S., Mohammadi, F., Nikaeen, M., Shamsizadeh, Z., Khazeni, A., Sahbaei, Z., Mousavi, S.M., Ghobadian, M., Mirhendi, H., 2021. COVID-19 infection risk from exposure to aerosols of wastewater treatment plants. Chemosphere 273, 129701. https://doi.org/10/gk3kg5

Gundy, P.M., Gerba, C.P., Pepper, I.L., 2009. Survival of Coronaviruses in Water and Wastewater. Food Environ. Virol. 1, 10. https://doi.org/10/b6s6qq

Guo, X., Wu, P., Ding, W., Zhang, W., Li, L., 2014. Reduction and characterization of bioaerosols in a wastewater treatment station via ventilation. J. Environ. Sci. 26, 1575–1583. https://doi.org/10.1016/j.jes.2014.06.001

Haas, C.N., 2015. Microbial Dose Response Modeling: Past, Present, and Future. Environ. Sci. Technol. 49, 1245–1259. https://doi.org/10/f627nw

Haas, C.N., Rycroft, T., Bibby, K., Casson, L., 2017. Risks from Ebolavirus Discharge from Hospitals to Sewer Workers. Water Environ. Res. 89, 357–368. https://doi.org/10/gbgjtt

Haas, C.N., 2020. Coronavirus and Environmental Engineering Science. Environ. Eng. Sci. 37, 233–234. https://doi.org/10/gqmb3z

Haji Ali, B., Shahin, M.S., Masoumi Sangani, M.M., Faghihinezhad, M., Baghdadi, M., 2021. Wastewater aerosols produced during flushing toilets, WWTPs, and irrigation with reclaimed municipal wastewater as indirect exposure to SARS-CoV-2. J. Environ. Chem. Eng. 9, 106201. https://doi.org/10/gm5h7t

Han, M.S., Seong, M.-W., Heo, E.Y., Park, J.H., Kim, N., Shin, S., Cho, S.I., Park, S.S., Choi, E.H., 2020. Sequential Analysis of Viral Load in a Neonate and Her Mother Infected With Severe Acute Respiratory Syndrome Coronavirus 2. Clin. Infect. Dis. 71, 2236–2239. https://doi.org/10/ggv487

Haque, S.E., Rahman, M., 2020. Association between temperature, humidity, and COVID-19 outbreaks in Bangladesh. Environ. Sci. Policy 114, 253–255. https://doi.org/10/ghrf47

Hart, O.E., Halden, R.U., 2020. Computational analysis of SARS-CoV-2/COVID-19 surveillance by wastewater-based epidemiology locally and globally: Feasibility,

economy, opportunities and challenges. Sci. Total Environ. 730, 138875. https://doi.org/10/ds22

Hasan, S.W., Ibrahim, Y., Daou, M., Kannout, H., Jan, N., Lopes, A., Alsafar, H., Yousef, A.F., 2021. Detection and quantification of SARS-CoV-2 RNA in wastewater and treated effluents: Surveillance of COVID-19 epidemic in the United Arab Emirates. Sci. Total Environ. 764, 142929. https://doi.org/10/gk3kh3

Hata, A., Honda, R., 2020. Potential Sensitivity of Wastewater Monitoring for SARS-CoV-2: Comparison with Norovirus Cases. Environ. Sci. Technol. 54, 6451–6452. https://doi.org/10/ggx23h

Heller, L., Mota, C.R., Greco, D.B., 2020. COVID-19 faecal-oral transmission: Are we asking the right questions? Sci. Total Environ. 729, 138919. https://doi.org/10/ggvq6g

Jahne, M.A., Rogers, S.W., Holsen, T.M., Grimberg, S.J., Ramler, I.P., 2015. Emission and Dispersion of Bioaerosols from Dairy Manure Application Sites: Human Health Risk Assessment. Environ. Sci. Technol. 49, 9842–9849. https://doi.org/10.1021/acs.est.5b01981

Jensen, K.S., Adams, R., Bennett, R.S., Bernbaum, J., Jahrling, P.B., Holbrook, M.R., 2018. Development of a novel real-time polymerase chain reaction assay for the quantitative detection of Nipah virus replicative viral RNA. PLOS ONE 13, e0199534. https://doi.org/10/gdqq69

Kassem, A.Z.E., 2020. Does Temperature Affect COVID-19 Transmission? Front. Public Health 8, 554964. https://doi.org/10/gk7m5m

Kataki, S., Patowary, R., Chatterjee, S., Vairale, M.G., Sharma, S., Dwivedi, S.K., Kamboj, D.V., 2022. Bioaerosolization and pathogen transmission in wastewater treatment plants: Microbial composition, emission rate, factors affecting and control measures. Chemosphere 287, 132180. https://doi.org/10.1016/j.chemosphere.2021.132180

Korzeniewska, E., Filipkowska, Z., Gotkowska-Płachta, A., Janczukowicz, W., Dixon, B., Czułowska, M., 2009. Determination of emitted airborne microorganisms from a BIO-PAK wastewater treatment plant. Water Res. 43, 2841–2851. https://doi.org/10.1016/j.watres.2009.03.050

Korzeniewska, E., 2011. Emission of bacteria and fungi in the air from wastewater treatment plants - a review. Front. Biosci. S3, 393–407. https://doi.org/10.2741/s159

Kweinor Tetteh, E., Opoku Amankwa, M., Armah, E.K., Rathilal, S., 2020. Fate of COVID-19 Occurrences in Wastewater Systems: Emerging Detection and Treatment Technologies—A Review. Water 12, 2680. https://doi.org/10/gqmb4m

Lou, M., Liu, S., Gu, C., Hu, H., Tang, Z., Zhang, Y., Xu, C., Li, F., 2021. The bioaerosols emitted from toilet and wastewater treatment plant: a literature review. Environ. Sci. Pollut. Res. 28, 2509–2521. https://doi.org/10/gqmb34

Lv, Q., Liu, M., Qi, F., Gong, S., Zhou, S., Zhan, S., Bao, L., 2020. Sensitivity of SARS‐CoV‐2 to different temperatures. Anim. Models Exp. Med. 3, 316‐318. https://doi.org/10/gk4ppf

Mandal, C.C., Panwar, M.S., 2020. Can the summer temperatures reduce COVID-19 cases? Public Health 185, 72–79. https://doi.org/10/ghjhkr

Marr, L.C., Tang, J.W., Van Mullekom, J., Lakdawala, S.S., 2019. Mechanistic insights into the effect of humidity on airborne influenza virus survival, transmission and incidence. J. R. Soc. Interface 16, 20180298. https://doi.org/10/gqmb47

Michałkiewicz, M., 2019. Wastewater Treatment Plants as a Source of Bioaerosols. Pol. J. Environ. Stud. 28, 2261–2271. https://doi.org/10/gmk55x

Ministry of Environmental Protection. 2013. Exposure Factors Handbook of Chinese Population. China Environmental Press, Beijing.

Mizukoshi, A., Nakama, C., Okumura, J., Azuma, K., 2021. Assessing the risk of COVID-19 from multiple pathways of exposure to SARS-CoV-2: Modeling in health-care settings and effectiveness of nonpharmaceutical interventions. Environ. Int. 147, 106338. https://doi.org/10/gjmzz2

Novel Coronavirus (2019-nCoV) situation report-1: Geneva: World Health Organization; 21 January 2020a.

Penn, R., Ward, B.J., Strande, L., Maurer, M., 2018. Review of synthetic human faeces and faecal sludge for sanitation and wastewater research. Water Res. 132, 222–240. https://doi.org/10/gc4c42

Pérez-López, F.R., Tajada, M., Savirón-Cornudella, R., Sánchez-Prieto, M., Chedraui, P., Terán, E., 2020. Coronavirus disease 2019 and gender-related mortality in European countries: A meta-analysis. Maturitas 141, 59–62. https://doi.org/10/gg4s8z

Polozov, I.V., Bezrukov, L., Gawrisch, K., Zimmerberg, J., 2008. Progressive ordering with decreasing temperature of the phospholipids of influenza virus. Nat. Chem. Biol. 4, 248–255. https://doi.org/10/dxn359

Randazzo, W., Truchado, P., Cuevas-Ferrando, E., Simón, P., Allende, A., Sánchez, G., 2020. SARS-CoV-2 RNA in wastewater anticipated COVID-19 occurrence in a low prevalence areas. Water Res. 181, 115942. https://doi.org/10/ggwtgc

Rimoldi, S.G., Stefani, F., Gigantiello, A., Polesello, S., Comandatore, F., Mileto, D., Maresca, M., Longobardi, C., Mancon, A., Romeri, F., Pagani, C., Cappelli, F., Roscioli, C., Moja, L., Gismondo, M.R., Salerno, F., 2020. Presence and infectivity of SARS-CoV-2 virus in wastewaters and rivers. Sci. Total Environ. 744, 140911. https://doi.org/10/gg4vnp

Saawarn, B., Hait, S., 2021. Occurrence, fate and removal of SARS-CoV-2 in wastewater: Current knowledge and future perspectives. J. Environ. Chem. Eng. 9, 104870. https://doi.org/10/gnnrfk

Sánchez-Monedero, M.A., Aguilar, M.I., Fenoll, R., Roig, A., 2008. Effect of the aeration system on the levels of airborne microorganisms generated at wastewater treatment plants. Water Res. 42, 3739–3744. https://doi.org/10.1016/j.watres.2008.06.028

Sarkar, J.P., Saha, I., Seal, A., Maity, D., Maulik, U., 2021. Topological Analysis for Sequence Variability: Case Study on more than 2K SARS-CoV-2 sequences of COVID-19 infected 54 countries in comparison with SARS-CoV-1 and MERS-CoV. Infect. Genet. Evol. 88, 104708. https://doi.org/10/gqmb33

Saththasivam, J., El-Malah, S.S., Gomez, T.A., Jabbar, K.A., Remanan, R., Krishnankutty, A.K., Ogunbiyi, O., Rasool, K., Ashhab, S., Rashkeev, S., Bensaad, M., Ahmed, A.A., Mohamoud, Y.A., Malek, J.A., Abu Raddad, L.J., Jeremijenko, A., Abu Halaweh, H.A., Lawler, J., Mahmoud, K.A., 2021. COVID-19 (SARS-CoV-2) outbreak monitoring using wastewater-based epidemiology in Qatar. Sci. Total Environ. 774, 145608. https://doi.org/10/gqmb32

Shi, K.-W., Wang, C.-W., Jiang, S.C., 2018. Quantitative microbial risk assessment of Greywater on-site reuse. Sci. Total Environ. 635, 1507–1519. https://doi.org/10/gqmp2p

Shi, P., Dong, Y., Yan, H., Zhao, C., Li, X., Liu, W., He, M., Tang, S., Xi, S., 2020. Impact of temperature on the dynamics of the COVID-19 outbreak in China. Sci. Total Environ. 728, 138890. https://doi.org/10/ggtxm4

Statement on the Second Meeting of the International Health Regulations (2005) Emergency Committee Regarding the Outbreak of Novel Coronavirus (2019-nCoV)：Geneva: World Health Organization; 2020b.

Tong, L., Ji, L., Li, D., Xu, H., 2022. The occurrence of COVID‐19 is associated with air quality and relative humidity. J. Med. Virol. 94, 965‐970. https://doi.org/10/gqfhvq

Usman, M., Farooq, M., Farooq, M., Anastopoulos, I., 2021. Exposure to SARS-CoV-2 in Aerosolized Wastewater: Toilet Flushing, Wastewater Treatment, and Sprinkler Irrigation. Water 13, 436. https://doi.org/10.3390/w13040436

van Doremalen, N., Bushmaker, T., Morris, D.H., Holbrook, M.G., Gamble, A., Williamson, B.N., Tamin, A., Harcourt, J.L., Thornburg, N.J., Gerber, S.I., Lloyd-Smith, J.O., de Wit, E., Munster, V.J., 2020. Aerosol and Surface Stability of SARS-CoV-2 as Compared with SARS-CoV-1. N. Engl. J. Med. 382, 1564–1567. https://doi.org/10/ggn88w

Wang, J., Tang, K., Feng, K., Lin, X., Lv, W., Chen, K., Wang, F., 2021. Impact of temperature and relative humidity on the transmission of COVID-19: a modelling study in China and the United States. BMJ Open 11, e043863. https://doi.org/10/gk7jgw

Wang, R., Alamin, Md., Tsuji, S., Hara-Yamamura, H., Hata, A., Zhao, B., Ihara, M., Honda, R., 2022. Removal performance of SARS-CoV-2 in wastewater treatment by membrane bioreactor, anaerobic-anoxic-oxic, and conventional activated sludge processes. Sci. Total Environ. 851, 158310. https://doi.org/10/gqrgfp

Wang, S.P., Gao, J.F., 2011. Process design manual of sewage treatment plant (Ⅱ).

Wang, W., Xu, Y., Gao, R., Lu, R., Han, K., Wu, G., Tan, W., 2020. Detection of SARS-CoV-2 in Different Types of Clinical Specimens. JAMA 323, 1843–1844. https://doi.org/10.1001/jama.2020.3786

Watanabe, T., Bartrand, T.A., Weir, M.H., Omura, T., Haas, C.N., 2010. Development of a Dose-Response Model for SARS Coronavirus: Dose-Response Model for SARS-CoV. Risk Anal. 30, 1129–1138. https://doi.org/10/d7gh8k

Westrell, T., Schönning, C., Stenström, T.A., Ashbolt, N.J., 2004. QMRA (quantitative microbial risk assessment) and HACCP (hazard analysis and critical control points)

for management of pathogens in wastewater and sewage sludge treatment and reuse. Water Sci. Technol. 50, 23–30. https://doi.org/10/gqmb6k

Wölfel, R., Corman, V.M., Guggemos, W., Seilmaier, M., Zange, S., Müller, M.A., Niemeyer, D., Jones, T.C., Vollmar, P., Rothe, C., Hoelscher, M., Bleicker, T., Brünink, S., Schneider, J., Ehmann, R., Zwirglmaier, K., Drosten, C., Wendtner, C., 2020. Virological assessment of hospitalized patients with COVID-2019. Nature 581, 465–469. https://doi.org/10.1038/s41586-020-2196-x

Wu, Y., Guo, C., Tang, L., Hong, Z., Zhou, J., Dong, X., Yin, H., Xiao, Q., Tang, Y., Qu, X., Kuang, L., Fang, X., Mishra, N., Lu, J., Shan, H., Jiang, G., Huang, X., 2020. Prolonged presence of SARS-CoV-2 viral RNA in faecal samples. Lancet Gastroenterol. Hepatol. 5, 434–435. https://doi.org/10/ggq8zp

Xu, Y., Li, X., Zhu, B., Liang, H., Fang, C., Gong, Y., Guo, Q., Sun, X., Zhao, D., Shen, J., Zhang, H., Liu, H., Xia, H., Tang, J., Zhang, K., Gong, S., 2020. Characteristics of pediatric SARS-CoV-2 infection and potential evidence for persistent fecal viral shedding. Nat. Med. 26, 502–505. https://doi.org/10.1038/s41591-020-0817-4

Zaneti, R.N., Girardi, V., Spilki, F.R., Mena, K., Westphalen, A.P.C., da Costa Colares, E.R., Pozzebon, A.G., Etchepare, R.G., 2021. Quantitative microbial risk assessment of SARS-CoV-2 for workers in wastewater treatment plants. Sci. Total Environ. 754, 142163. https://doi.org/10/gm5h2w

Zhang, N., Gong, Y., Meng, F., Bi, Y., Yang, P., Wang, F., 2020. Virus shedding patterns in nasopharyngeal and fecal specimens of COVID-19 patients (preprint). Infectious Diseases (except HIV/AIDS). https://doi.org/10.1101/2020.03.28.20043059

Zhang, X., Wu, J., Smith, L.M., Li, X., Yancey, O., Franzblau, A., Dvonch, J.T., Xi, C., Neitzel, R.L., 2022. Monitoring SARS-CoV-2 in air and on surfaces and estimating infection risk in buildings and buses on a university campus. J. Expo. Sci. Environ. Epidemiol. https://doi.org/10/gp4dxd

Zhou, L., Echigo, S., Ohkouchi, Y., Itoh, S., 2014. Quantitative microbial risk assessment of drinking water treated with advanced water treatment process. J. Water Supply Res. Technol.-Aqua 63, 114–123. https://doi.org/10/f5wwn7

8-6 average relative humidity of main cities, 2020. China Statistical Yearbook.

Supplementary Material

Supplementary Material Table 1. References for data of SARS-CoV-2 concentrations in stool

SARS-CoV-2 load	References
$1.7\times10^6 - 4.1\times10^7$ genomes/ml	Han et al., 2020
$10^{3.4}$–$10^{7.6}$ genomes/ml	Cheung et al., 2020
10^3–10^7 genomes /g	Wolfel et al., 2020
5623 genomes/ml (mean) $10^{5.8}$ genomes/ml (peak)	Zhang et al., 2020
$<2.6\times10^4$ genomes/ml	Wang et al., 2020
2×10^3–2×10^7 genomes/ml	Xu et al., 2020
8.01×10^6 genomes/g (mean)	Anjos et al., 2022

Supplementary Material Table 2. Seasonal temperature in different environmental conditions (°C)

Environmental condition	Spring	Summer	Autumn	Winter
Hot and humid	20 ± 10	30 ± 10	20 ± 10	5 ± 5
Hot and dry	20 ± 10	25 ± 5	15 ± 15	5 ± 5
Mild and humid	15 ± 5	25 ± 5	15 ± 5	10 ± 10
Mild and dry	10 ± 10	15 ± 5	10 ± 10	0 ± 10
Cold and humid	10 ± 10	15 ± 15	0 ± 10	-10 ± 5
Cold and dry	10 ± 10	15 ± 15	0 ± 10	-5 ± 5

Data refer the seasonal temperature of main cities in China (China Statistical Yearbook, 2020).

Supplementary Material Table 3. Seasonal relative humidity in different environmental conditions (%)

Environmental condition	Spring	Summer	Autumn	Winter
Hot and humid	75 ± 5	80 ± 10	70 ± 10	85 ± 5
Hot and dry	45 ± 15	55 ± 15	55 ± 5	50 ± 10
Mild and humid	55 ± 5	75 ± 15	75 ± 5	60 ± 10
Mild and dry	30 ± 10	45 ± 15	45 ± 15	25 ± 5
Cold and humid	50 ± 10	75 ± 15	60 ± 10	60 ± 20
Cold and dry	35 ± 5	55 ± 15	55 ± 5	50 ± 20

Data refer the seasonal relative humidity of main cities in China (China Statistical Yearbook, 2020).

Supplementary Material Table 4. Daily probability of infection ($P_i(d)$) of various exposure scenarios in the four seasons exposing to bioaerosol inhalation exposure pathway

Items			Environmental condition											
			Hot & humid		Hot & dry		Mild & humid		Mild & dry		Cold & humid		Cold & dry	
			Best	Worst	Best	Worst	Best	Worst	Best	Worst	Best	Worst	Best	Worst
Spring	Male	5th percentile	2.89×10^{-5}	2.94×10^{-3}	3.81×10^{-5}	3.70×10^{-3}	3.89×10^{-5}	3.99×10^{-3}	4.27×10^{-5}	4.35×10^{-3}	4.26×10^{-5}	4.15×10^{-3}	4.57×10^{-5}	4.43×10^{-3}
		Median	1.71×10^{-4}	1.68×10^{-2}	2.19×10^{-4}	2.14×10^{-2}	2.28×10^{-4}	2.27×10^{-2}	2.57×10^{-4}	2.49×10^{-2}	2.45×10^{-4}	2.42×10^{-2}	2.54×10^{-4}	2.50×10^{-2}
		95th percentile	3.89×10^{-4}	3.79×10^{-2}	4.20×10^{-4}	4.07×10^{-2}	4.20×10^{-4}	4.13×10^{-2}	4.72×10^{-4}	4.61×10^{-2}	4.48×10^{-4}	4.38×10^{-2}	4.66×10^{-4}	4.57×10^{-2}
	Female	5th percentile	2.30×10^{-5}	2.34×10^{-3}	3.03×10^{-5}	2.94×10^{-3}	3.09×10^{-5}	3.17×10^{-3}	3.39×10^{-5}	3.46×10^{-3}	3.39×10^{-5}	3.30×10^{-3}	3.63×10^{-5}	3.52×10^{-3}
		Median	1.36×10^{-4}	1.34×10^{-2}	1.74×10^{-4}	1.70×10^{-2}	1.81×10^{-4}	1.81×10^{-2}	2.04×10^{-4}	1.98×10^{-2}	1.95×10^{-4}	1.93×10^{-2}	2.02×10^{-4}	2.00×10^{-2}
		95th percentile	3.09×10^{-4}	3.02×10^{-2}	3.34×10^{-4}	3.25×10^{-2}	3.34×10^{-4}	3.30×10^{-2}	3.75×10^{-4}	3.68×10^{-2}	3.56×10^{-4}	3.50×10^{-2}	3.71×10^{-4}	3.65×10^{-2}
Summer	Male	5th percentile	1.90×10^{-5}	1.86×10^{-3}	3.18×10^{-5}	3.15×10^{-3}	2.61×10^{-5}	2.68×10^{-3}	3.96×10^{-5}	3.98×10^{-3}	3.12×10^{-5}	2.97×10^{-3}	3.68×10^{-5}	3.56×10^{-3}
		Median	1.13×10^{-4}	1.10×10^{-2}	1.87×10^{-4}	1.83×10^{-2}	1.52×10^{-4}	1.53×10^{-2}	2.37×10^{-4}	2.31×10^{-2}	1.79×10^{-4}	1.78×10^{-2}	2.05×10^{-4}	2.03×10^{-2}
		95th percentile	2.91×10^{-4}	2.86×10^{-2}	3.60×10^{-4}	3.50×10^{-2}	3.07×10^{-4}	3.01×10^{-2}	4.38×10^{-4}	4.26×10^{-2}	3.67×10^{-4}	3.60×10^{-2}	4.00×10^{-4}	3.91×10^{-2}
	Female	5th percentile	1.51×10^{-5}	1.48×10^{-3}	2.53×10^{-5}	2.51×10^{-3}	2.08×10^{-5}	2.13×10^{-3}	3.14×10^{-5}	3.17×10^{-3}	2.48×10^{-5}	2.75×10^{-3}	2.93×10^{-5}	2.83×10^{-3}
		Median	8.95×10^{-5}	8.75×10^{-3}	1.49×10^{-4}	1.46×10^{-2}	1.21×10^{-4}	1.22×10^{-2}	1.88×10^{-4}	1.84×10^{-2}	1.42×10^{-4}	1.63×10^{-2}	1.63×10^{-4}	1.62×10^{-2}
		95th percentile	2.31×10^{-4}	2.28×10^{-2}	2.86×10^{-4}	2.79×10^{-2}	2.44×10^{-4}	2.40×10^{-2}	3.48×10^{-4}	3.40×10^{-2}	2.91×10^{-4}	3.12×10^{-2}	3.18×10^{-4}	3.12×10^{-2}
Autumn	Male	5th percentile	3.05×10^{-5}	3.08×10^{-3}	3.79×10^{-5}	3.72×10^{-3}	3.56×10^{-5}	3.63×10^{-3}	4.08×10^{-5}	4.19×10^{-3}	4.27×10^{-5}	4.08×10^{-3}	4.43×10^{-5}	4.25×10^{-3}
		Median	1.79×10^{-4}	1.75×10^{-2}	2.19×10^{-4}	2.14×10^{-2}	2.09×10^{-4}	2.08×10^{-2}	2.46×10^{-4}	2.39×10^{-2}	2.46×10^{-4}	2.44×10^{-2}	2.46×10^{-4}	2.45×10^{-2}
		95th percentile	4.02×10^{-4}	3.91×10^{-2}	4.29×10^{-4}	4.19×10^{-2}	3.87×10^{-4}	3.82×10^{-2}	4.57×10^{-4}	4.45×10^{-2}	4.59×10^{-4}	4.47×10^{-2}	4.62×10^{-4}	4.53×10^{-2}
	Female	5th percentile	2.42×10^{-5}	2.45×10^{-3}	3.01×10^{-5}	2.96×10^{-3}	2.83×10^{-5}	2.89×10^{-3}	3.24×10^{-5}	3.33×10^{-3}	3.40×10^{-5}	3.25×10^{-3}	3.52×10^{-5}	3.38×10^{-3}
		Median	1.42×10^{-4}	1.39×10^{-2}	1.74×10^{-4}	1.71×10^{-2}	1.66×10^{-4}	1.66×10^{-2}	1.95×10^{-4}	1.90×10^{-2}	1.96×10^{-4}	1.94×10^{-2}	1.96×10^{-4}	1.95×10^{-2}
		95th	3.20×10^{-4}	3.12×10^{-2}	3.41×10^{-4}	3.34×10^{-2}	3.07×10^{-4}	3.05×10^{-2}	3.63×10^{-4}	3.56×10^{-2}	3.64×10^{-4}	3.57×10^{-2}	3.67×10^{-4}	3.61×10^{-2}

		percentile												
Winter	Male	5th percentile	3.88×10^{-5}	3.91×10^{-3}	4.32×10^{-5}	4.25×10^{-3}	4.00×10^{-5}	4.11×10^{-3}	4.47×10^{-5}	4.54×10^{-3}	4.75×10^{-5}	4.60×10^{-3}	4.75×10^{-5}	4.60×10^{-3}
		Median	2.30×10^{-4}	2.23×10^{-2}	2.54×10^{-4}	2.49×10^{-2}	2.35×10^{-4}	2.34×10^{-2}	2.69×10^{-4}	2.61×10^{-2}	2.74×10^{-4}	2.69×10^{-2}	2.66×10^{-4}	2.62×10^{-2}
		95th percentile	4.84×10^{-4}	4.70×10^{-2}	4.69×10^{-4}	4.53×10^{-2}	4.40×10^{-4}	4.30×10^{-2}	4.94×10^{-4}	4.81×10^{-2}	4.97×10^{-4}	4.85×10^{-2}	4.89×10^{-4}	4.77×10^{-2}
	Female	5th percentile	3.08×10^{-5}	3.11×10^{-3}	3.44×10^{-5}	3.38×10^{-3}	3.18×10^{-5}	3.27×10^{-3}	3.55×10^{-5}	3.61×10^{-3}	3.78×10^{-5}	3.65×10^{-3}	3.77×10^{-5}	3.66×10^{-3}
		Median	1.83×10^{-4}	1.78×10^{-2}	2.02×10^{-4}	1.98×10^{-2}	1.86×10^{-4}	1.87×10^{-2}	2.14×10^{-4}	2.08×10^{-2}	2.18×10^{-4}	2.15×10^{-2}	2.11×10^{-4}	2.09×10^{-2}
		95th percentile	3.85×10^{-4}	3.75×10^{-2}	3.73×10^{-4}	3.62×10^{-2}	3.49×10^{-4}	3.43×10^{-2}	3.93×10^{-4}	3.84×10^{-2}	3.95×10^{-4}	3.87×10^{-2}	3.89×10^{-4}	3.81×10^{-2}

5th percentile= imprudent estimate

Median= moderate estimate

95th percentile= conservative estimate

Best= best-case scenario (0.03% of the population are infected)

Worst= worst-case scenario (3% of the population are infected)

Supplementary Material Table 5. Daily probability of infection ($P_i(d)$) of various exposure scenarios by direct droplet ingestion exposure pathway

	Best-case scenario	Worst-case scenario
5th percentile	9.56×10^{-5}	9.52×10^{-3}
Median	5.61×10^{-4}	5.46×10^{-2}
95th percentile	1.02×10^{-3}	9.74×10^{-2}

5th percentile= imprudent estimate

Median= moderate estimate

95th percentile= conservative estimate

Best-case scenario=0.03% of the population are infected

Worst-case scenario=3% of the population are infected

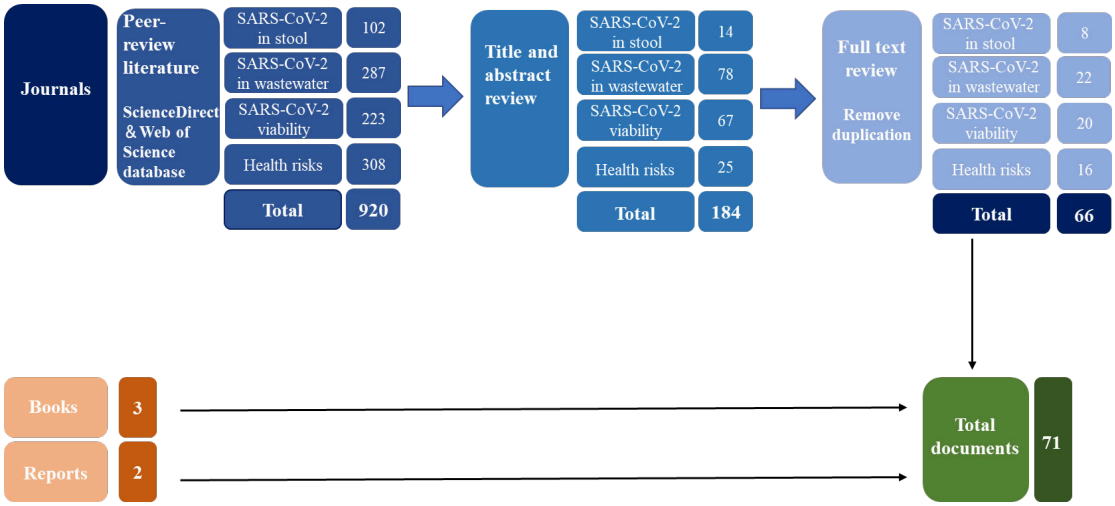

Supplementary Material Figure 1. Graphic illustrating terms used in literature research and selection of sources. Numbers are the number of documents assessed, with totals shown in a darker shade.

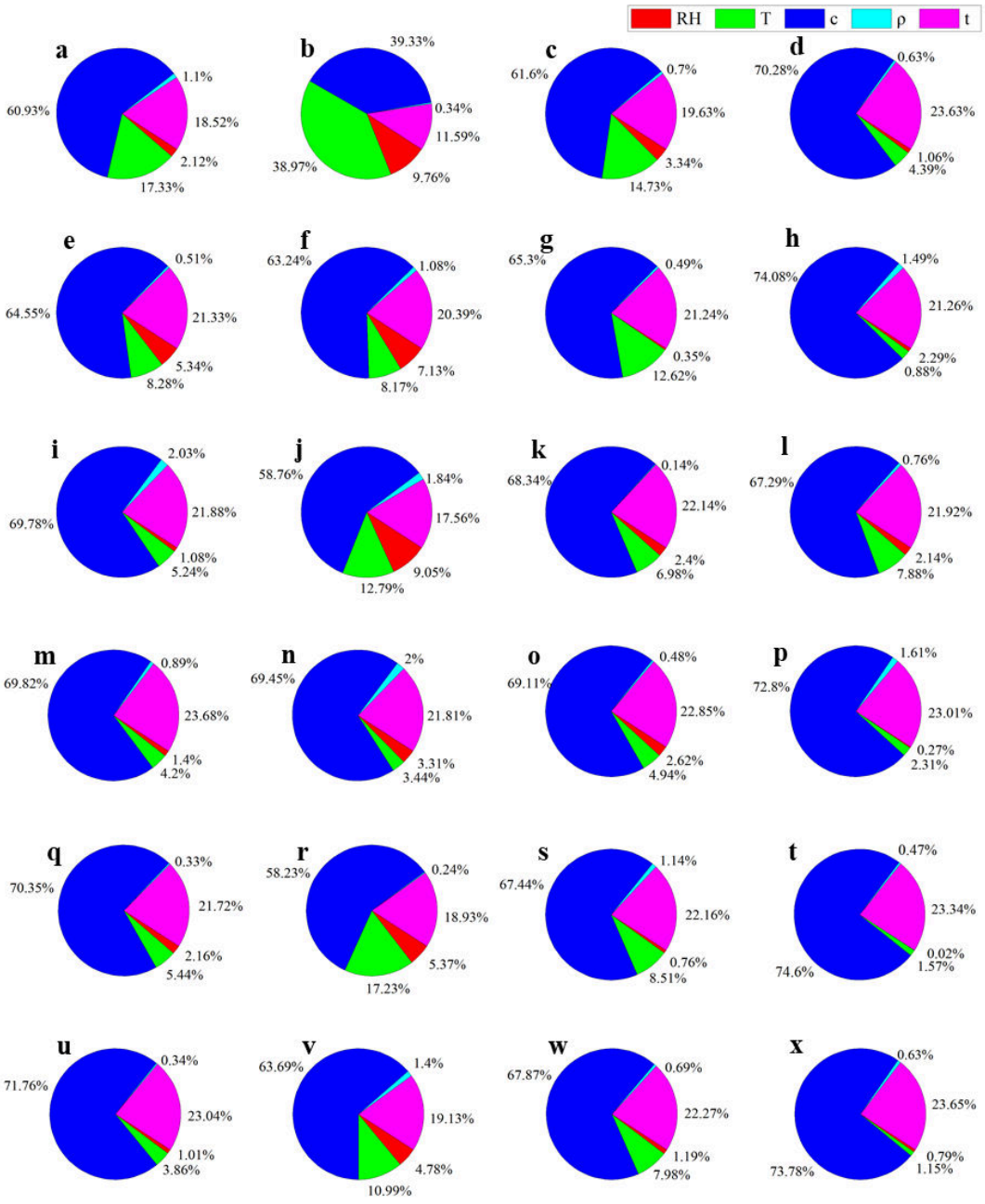

Supplementary Material Figure 2. Pie charts showing the specific contribution of variance of input variables that impact the output values of daily infection risk for the bioaerosol inhalation pathway in four seasons referring to six kinds of environmental conditions: (a) spring in hot and humid conditions, (b) summer in hot and humid conditions, (c) autumn in hot and humid conditions, (d) winter in hot and humid conditions, (e) spring in hot and dry conditions, (f) summer in hot and dry conditions, (g) autumn in hot and dry conditions, (h) winter in hot and dry conditions, (i) spring in mild and humid conditions, (j) summer in mild and humid conditions, (k) autumn in mild and humid conditions, (l) winter in mild and humid conditions, (m) spring in mild and dry conditions, (n) summer in mild and dry conditions, (o) autumn in mild and dry conditions, (p) winter in mild and dry conditions, (q) spring in cold and humid

conditions, (r) summer in cold and humid conditions, (s) autumn in cold and humid conditions, (t) winter in cold and humid conditions, (u) spring in cold and dry conditions, (v) summer in cold and dry conditions, (w) autumn in cold and dry conditions, and (x) winter in cold and dry conditions. (*c*: Concentrations of SARS-CoV-2 in stool; *t*: Exposure time; *T*: Temperature; *RH*: Relative humidity; ρ: Density of stool).

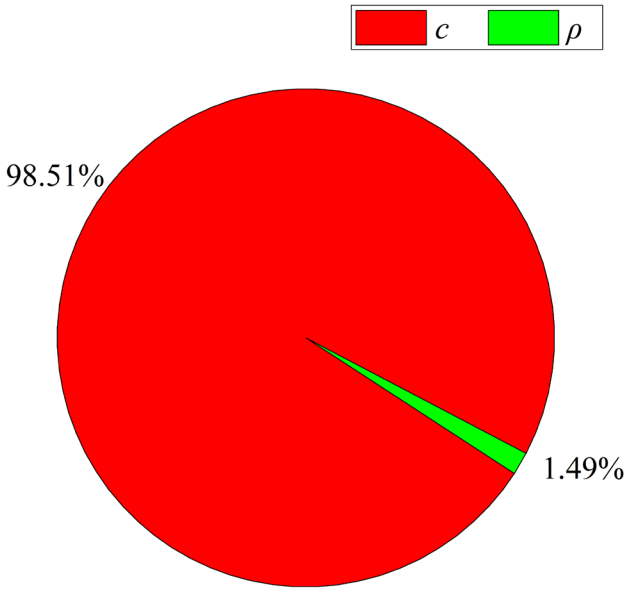

Supplementary Material Figure 3. Pie chart to display the contribution to variance of input variables that impact the output values for the direct droplet ingestion pathway. (*c*: Concentrations of SARS-CoV-2 in stool; ρ: Density of stool).

Quantitative SARS-CoV-2 exposure assessment for workers in wastewater treatment plants using Monte-Carlo simulation

Yan, Cheng

2023-11-16

Yan C, Hu YN, Gui ZC, et al., (2024) Quantitative SARS-CoV-2 exposure assessment for workers in wastewater treatment plants using Monte-Carlo simulation. Water Research, Volume 248, January 2024, Article number 120845

https://doi.org/10.1016/j.watres.2023.120845